



ELSEVIER

Available online at [www.sciencedirect.com](http://www.sciencedirect.com)

Procedia Engineering 5 (2010) 1401–1404

---

---

**Procedia  
Engineering**

---

---

[www.elsevier.com/locate/procedia](http://www.elsevier.com/locate/procedia)

Proc. EuroSensors XXIV, September 5-8, 2010, Linz, Austria

## Magnetic flux leakage measurement setup for defect detection

Johannes Atzlesberger<sup>a\*</sup>, Bernhard Zagar<sup>a</sup><sup>a</sup>*Institute for Measurement Technology, Altenbergerstrasse 69, Linz 4040, Austria*

---

### Abstract

This paper describes a potential technique to detect medium size defects in ferromagnetic specimen by using rather inexpensive but highly sensitive sensors based on the giant magneto resistive effect (GMR) [1]. The sensor effect is used very effectively in ultra high density magnetic recording devices and might thus prove effective in the material testing business, too. These sensors measure the magnetic flux leakage near the surface of a magneto-conductive object. In order to test their potential initial tests were performed and their results evaluated. For this survey some test specimen were made by intentionally causing some imperfections (actually small drilled holes, or some surface scratches, etc.) in an otherwise homogeneous and isotropic ferromagnetic specimen. In order to obtain the distribution of the magnetic flux leakage, the surface of the test specimen was mechanically scanned. Preliminary results are very encouraging since we could show that even small blemishes can easily be detected this way.

© 2010 Published by Elsevier Ltd. Open access under [CC BY-NC-ND license](https://creativecommons.org/licenses/by-nc-nd/4.0/).

Keywords: Magnetic Flux Leakage (MFL); Giant Magneto Resistor (GMR); Defect Detection; Non-Destructive Testing (NDT);

---

### 1. Magnetic Flux Leakage

Figure 1 illustrates the principle of the magnetic flux leakage method [2]. An electromagnet induces a magnetic flux which is modulated by the inhomogeneities in the specimen. This modulation causes a field displacement sufficiently large that a properly positioned sensor (in particular it needs to be close to the scanned surface) can easily detect.

### 2. Sensors

For our initial experiments various types of sensors arrangements were tested for efficacy. In particular a magnetometer (AA002-02) and a gradiometer (AB001-02) fabricated by NVE ([www.nve.com](http://www.nve.com)) were used throughout the measurements. These sensors effectively form a measurement bridge circuit of four GMR-resistors

---

\* Corresponding author. Tel.: +43-732-2468-9216; fax: +43-732-2468-9233.  
E-mail address: [Johannes.Atzlesberger@jku.at](mailto:Johannes.Atzlesberger@jku.at).

and are more sensitive and cheaper than typically used sensors like AMR-sensors (anisotropic magneto resistor). Due to their particular design the sensors have a sensitive axis and an orthogonally oriented nonsensitive axis. The magnetometer's characteristic hysteresis curve was measured by positioning the sensor in the center of a Helmholtz coil. (In the center of a Helmholtz coil the magnetic field is homogeneous and easily determined from the drive current and geometrical parameters. If the currents in the two coils are oriented in different directions a Maxwell coil arrangement results giving a constant gradient of the magnetic field as used later for measuring the gradiometer's characteristic.)

The magnetic flux density on the axis of symmetry ( $x$ -axis) caused by the Helmholtz coil pair can very precisely be calculated using Biot-Savart's law [3].

$$\vec{B}(x) = \frac{\mu_0 IN}{2} \cdot \frac{R^2}{(R^2 + x^2)^{\frac{3}{2}}} \cdot \vec{e}_x \quad (1)$$

With  $\mu_0$ , permeability of free space,  $I$ , excitation current,  $N$  number of turns and  $R$ , the distance as well as the radius of the coils.

Positioning the GMR-sensor in the center between the two coils, means that

$$x = \pm \frac{R}{2} \quad (2)$$

so Eqn. 1 can be rewritten to

$$\vec{B}\left(\pm \frac{R}{2}\right) = \frac{\mu_0 IN}{2} \cdot \frac{R^2}{\left(R^2 + \left(\pm \frac{R}{2}\right)^2\right)^{\frac{3}{2}}} \cdot \vec{e}_x \quad (3)$$

The magnetic field in the center of the Helmholtz coil pair can be calculated by the superposition of the two magnetic fields produced by the two coils:

$$\begin{aligned} \vec{B}_{tot} &= \vec{B}\left(\frac{R}{2}\right) + \vec{B}\left(-\frac{R}{2}\right) = 2\vec{B}\left(\frac{R}{2}\right) = \\ &= \mu_0 \cdot \frac{INR^2}{\left(R^2 + \frac{R^2}{4}\right)^{\frac{3}{2}}} \cdot \vec{e}_x = \mu_0 \cdot \frac{8 \cdot NI}{\sqrt{125}R} \cdot \vec{e}_x \end{aligned} \quad (5)$$

The magnetic field strength in air can be calculated as

$$\begin{aligned} \vec{H}_{tot} &= \frac{\vec{B}_{tot}}{\mu_0} \\ \vec{H}_{tot} &= \frac{8 \cdot NI}{\sqrt{125}R} \cdot \vec{e}_x \end{aligned} \quad (6)$$

In Fig. 2 the magnetometer's characteristic is shown for a magnetic field strength in the range of  $\pm 2600$  A/m for a sensor supply voltage of  $\pm 10$  V. Between 0 A/m and the saturation field of about 1200 A/m the characteristic is nearly linear. Within this linear range the operating point is placed symmetrically.

The magnetometer's characteristic hysteresis curve was measured by positioning the sensor in the center of a Maxwell coil pair. The magnetic field strength in air can be calculated using Biot-Savart's law and superposition the two magnetic fields produced by the two coils.

$$\vec{H}_{tot} = \left( \frac{-INR^2}{2\left(R^2 + \left(\frac{a}{2}\right)^2\right)^{\frac{3}{2}}} + \frac{INR^2}{2\left(R^2 + \left(-\frac{a}{2}\right)^2\right)^{\frac{3}{2}}} \right) \cdot \vec{e}_x \quad (7)$$

With  $I$ , excitation current,  $N$  number of turns,  $R$ , the radius of the coils and  $a$ , the distance between the coils. The derivative of the magnetic field strength with respect to location results in the gradient of the magnetic field strength.

$$\frac{d\vec{H}_{tot}}{dx} = \frac{INR^2}{2(R^2 + x^2)^{\frac{3}{2}}} - \frac{INR^2}{2\left(R^2 + \left(x + \frac{a}{2}\right)^2\right)^{\frac{3}{2}}} + \frac{INR^2}{2\left(R^2 + \left(x - \frac{a}{2}\right)^2\right)^{\frac{3}{2}}} + \frac{3}{4} \cdot \frac{INR^2(2x + a)}{\left(R^2 + \left(x + \frac{a}{2}\right)^2\right)^{\frac{5}{2}}} - \frac{3}{4} \cdot \frac{INR^2(2x - a)}{\left(R^2 + \left(x - \frac{a}{2}\right)^2\right)^{\frac{5}{2}}} \quad (8)$$

Figure 3 shows the gradiometer’s characteristic for a magnetic field strength gradient between  $-1 \text{ MA/m}^2$  and  $2.8 \text{ MA/m}^2$  for a sensor supply voltage of  $\pm 10 \text{ V}$ .

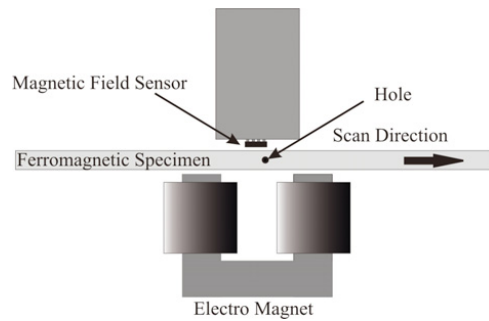


Fig. 1: Schematic test set-up of the magnetic flux leakage method.

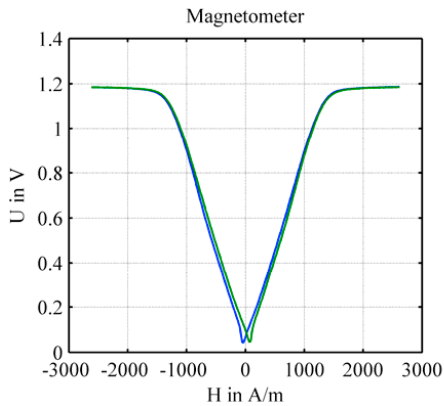


Fig. 2: Characteristic hysteresis curve of the GMR-magnetometer (AA002-02) with a supply voltage of  $U = \pm 10 \text{ V}$ .

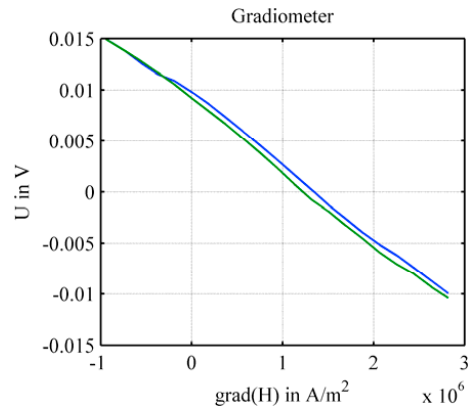


Fig. 3: Characteristic hysteresis curve of the GMR-gradiometer (AB001-02) with a supply voltage of  $U = \pm 10 \text{ V}$ .

### 3. Preliminary Test Results

A ferromagnetic specimen with blind holes partly filled by a magnetizable spiral drill and oriented parallel to its surface was scanned using both a GMR-magnetometer and a GMR-gradiometer type system. The result for the two-dimensional scan and a microscope image of a blind hole and a blind hole containing a broken spiral drill with a diameter of 0.5 mm are shown in Fig. 3(a). The photo in Fig. 3(b) shows the scanned part of the specimen, where the  $x$ -distance of 47.5 mm is marked. The results of a one-dimensional scan with the magnetometer and the gradiometer on this line are shown in Fig. 4. The peaks in the magnetometer signal and the steep flanks in the gradiometer signal indicate the positions of the holes correctly.

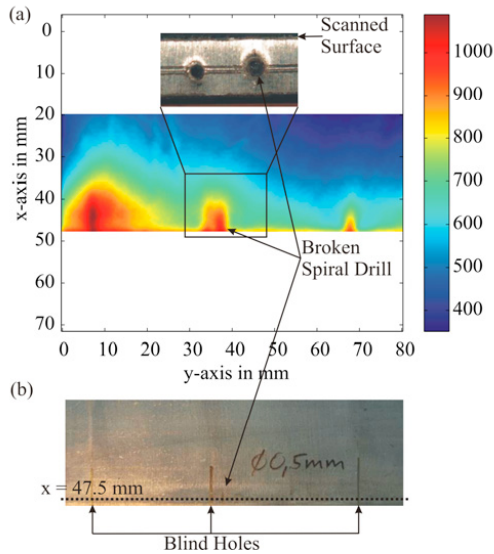


Fig. 4: The two-dimensional magnetometer scan of a ferromagnetic specimen containing blind holes partly filled by a broken magnetizable spiral drill inside a blind hole are shown in (a). The image in (b) shows a photo of the scanned part of the specimen.

#### 4. Conclusion

The test results obtained from the GMR-sensors are promising. In order to develop an automatic measuring system with a very high inspection speed for the industry, the measurement system will contain many of these sensors in an array. So the data acquisition and mainly the data evaluation will be a challenge since the system has to find defects that are greater than a particular value but be insensitive to false alarms caused by artefacts because this would produce high costs. Due to the very harsh environment in the industry the durability of the sensors might be a problem but solvable.

#### Acknowledgements

The authors gratefully acknowledge the partial financial support for the work presented in this paper by the Austrian Center of Competence in Mechatronics (ACCM).

#### References

- [1] Hauser H, Magnetoresistors. In : Ripka P, editor. *Magnetic Sensors and Magnetometers*, pp. 129-171, 2001, ISBN 3-8169-0964-7
- [2] Blitz J, *Electrical and Magnetic Methods of Non-destructive Testing*, 2<sup>nd</sup> Edition, 1997, ISBN 0-412-79150-1
- [3] Nicolet A, *Electric and Magnetic Fields – From Numerical Models to Industrial Application*, pp. 3-6, Belgium, 1994, ISBN 0-306-44991-9

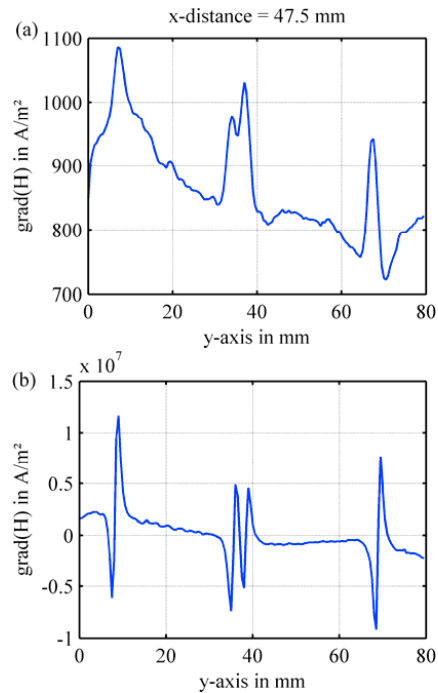


Fig. 5: The peaks in the magnetometer signal (a) and the steep flanks in the gradiometer signal (b) indicate the positions of the holes.